Effects of Low-Energy End Groups on the Dewetting Dynamics of Poly(styrene) Films on Poly(methyl methacrylate) Substrates

Caigen Yuan,† Meng Ouyang,‡ and Jeffrey T. Koberstein*

Department of Chemical Engineering and The Polymer Program, University of Connecticut, Storrs, Connecticut 06269-3136

Received May 14, 1998; Revised Manuscript Received January 19, 1999

ABSTRACT: The influence of surface-active fluorocarbon-terminated poly(styrene) (PS−F) additives on the dewetting dynamics of thin melt films of poly(styrene) (PS) deposited onto poly(methyl methacrylate) (PMMA) substrates is investigated by reflection optical microscopy. The dewetting velocity is found to be time invariant and decreases with increase in PS−F content. Dewetting is completely eliminated for the neat PS−F films. The surface tension reduction due to PS−F addition is characterized by analysis of water contact angles on the PS blends and by measurement of equilibrium contact angles for droplets of the dewetted blends on PMMA by atomic force microscopy. Increasing the PS−F content decreases the PS blend surface tension and reduces its equilibrium contact angle on PMMA. Lower molecular weight PS−F is more effective in reducing the dewetting velocity owing to its higher fluorocarbon content and subsequently larger reduction in surface tension. The dependence of dewetting velocity (V) on the PS blend viscosity (η), surface tension (γ), and contact angle on PMMA (θ_E) is in excellent agreement with the relationship $V = \gamma(\theta_E)^3/(12L\eta\sqrt{2})$ proposed by Brochard-Wyart, Martin, and Redon (BMR). The value of the prefactor L is found to be 16.4 for both series of blends, similar in magnitude to previously reported values for poly(dimethylsiloxane).

Introduction

The stabilization of polymer thin films against dewetting is of great importance to a number of technological applications. The likelihood of liquid films to either wet or dewet solid surfaces is related to the value of the spreading parameter S:

$$S = \gamma_B - (\gamma_A + \gamma_{AB}) \quad (1)$$

where γ_A and γ_B are the surface tension of liquid (A) and solid substrate (B), and γ_{AB} is the AB interfacial tension. If S is positive, A spreads on B; if S is negative, A dewets B.

Polymer films can be coated onto even nonwetting substrates using techniques such as spin-coating; however, these thin films are often only metastable and will dewet when heated above their glass transition temperatures. The wetting and dewetting behavior of thin polymer films on different types of substrates including silicon wafers and solid polymers has been studied both theoretically[1−6] and experimentally[7−15] for many years.

Much recent interest has focused on the use of functional additives to control the wetting behavior of thin polymer films. Henn et al.[16] reported the wetting and dewetting behavior of thin films of end-functional polymers, ω- and α,ω-barium sulfonatopolystyrene, on silicon substrates. Low molecular weight monofunctional chains were found to dewet the substrate similar to normal polystyrene; however, the entire silicon substrate remained covered by a monolayer of monofunctional chains after dewetting. High molecular weight monofunctional chains and difunctional chains did not dewet the silicon substrate.

Yerushalmi and Klein[17] discussed the stabilization of a low molecular weight polystyrene by polymeric additives. They observed that addition of long polystyrene chains up to a concentration of 10% did not change the wetting behavior of styrene oligomers but that end-functional polystyrene, together with some free long polystyrene chains in the liquid, stabilized the films. They suggested that the stabilization of these films arises from the formation of an entanglement network between the free chains and surface tethered brush molecules. The end-functional polymers employed in these two cases produce polymer brushes at the polymer−solid interface due to anchoring of the end group on the substrate.

There has also been recent interest in the dewetting of polymer films on polymeric substrates. Brochard-Wyart, Martin, and Redon (BMR)[1] presented a theoretical study of the dewetting mechanisms of a molten polymer deposited on a second, immiscible, polymer melt. They considered the influence of the relative viscosities of the two melts, the thickness of the respective layers, and the interfacial tensions involved. Qu et al.[15] reported experiments of dewetting dynamics of thin PS films on PMMA substrates as a function of the molecular weights of the two materials. For high PMMA molecular weights, the lower layer is solidlike, while for low molecular weights, the lower layer is liquidlike during the dewetting process. Their results compared favorably with the predictions of BMR theory.

We report herein the effects of low-energy fluorocarbon chain ends on the wetting and dewetting properties of PS films on a PMMA substrate. It is now well-known that surface properties of polymer melts such as surface tension are strongly influenced by the nature of the polymer end group.[18−22] Fluorocarbon chain ends on PS segregate preferentially to the surface, causing a reduc-

* To whom correspondence should be addressed.
† Current address: Institute of Petrochemical Engineering, East China University of Science and Technology, Jin-Shan Wei, Shanghai 200540, P. R. China.
‡ Current address: Department of Materials Science, University of Pennsylvania, Philadelphia, PA 19104.

10.1021/ma980774o CCC: $18.00
Published on Web 03/04/1999

Table 1. Characteristics of the Polymers Used in This Study

polymer[a]	M_w	M_w/M_n
PMMA	100 000	1.66
PS34.5K	34 500	1.05
PS−F35.5K	35 500	1.05
PS−F17.3K	17 300	1.16
PS−F5.4K	5 400	1.12

[a] PS−F designates fluorocarbon end-functional polystyrene terminated with $-Si(CH_3)_2-CH_2-CH_2-(CF_2)_5-CF_3$.

tion in surface tension that can be controlled by changing the polymer molecular weight and bulk concentration of fluorocarbon end-functional polystyrene.[23−26] These polymers are used to systematically investigate the dewetting dynamics of polymer thin films as a means of verifying the BMR theory.

Experimental Section

End-functional polystyrene (PS−F) with the fluorocarbon end group $[Si(CH_3)_2-CH_2-CH_2-(CF_2)_5CF_3]$ was synthesized by anionic polymerization of styrene initiated with *sec*-butyllithium and terminated by a fluorinated chlorosilane. Molecular weight and molecular weight distribution were measured by gel permeation chromatography using toluene as solvent and polystyrene calibration standards. Poly(methyl methacrylate) (PMMA100K) was purchased from Polysciences. Polystyrene (PS34.5K) was purchased from Polymer Laboratories. The characteristics of the polymers used are given in Table 1.

Polished silicon wafers were ultrasonically cleaned in chloroform to remove dust and irradiated by UV ozone prior to use to remove organic contaminants. PMMA overlayers with a nominal thickness of 52 nm were deposited by spin-coating from a 10 mg/mL solution in toluene onto clean silicon wafers that were subsequently dried in a vacuum oven to remove residual solvent. The film thickness was measured with a J.A. Woollam ellipsometer. Blends of PS−F with PS34.5K were prepared by codissolution in cyclohexane. Thin PS blend films were directly spin-coated onto PMMA to form bilayers. The PS film thickness was approximately 60 nm.

The dewetting experiments were carried out by annealing the bilayer polymer films in a vacuum at 165 °C. Photomicrographs of different stages of dewetting were taken with a Nikon optical microscope in reflection mode.

The contact angles of water on PS blend films were measured using a computer-automated contact angle tensiometer (Material Interface Associates, Inc. design) with Millipore water as the sessile drop fluid. The tensiometer was constructed in house and is based upon the collection of digital images of sessile drops. The contact angle was determined by regression of the modified LaPlace equations to the entire sessile drop shape. The contact angle is subsequently calculated by integration of the best fit differential equations that characterize the drop shape. The general procedures employed and the device utilized are similar to those previously reported for pendant drop shape analysis.[27] Typical analyses of advancing and receding angles used in many investigations are not useful in the present case because of surface rearrangement caused by the presence of water.[28] The reported water contact angles represent initial "equilibrium" values that are determined by forming a drop under advancing conditions and then waiting several minutes to allow local equilibration before collecting drop images. Under these conditions, the drop shape comes to equilibrium, but significant restructuring of the interphase does not occur. We have found that this procedure gives data on surface composition that are consistent with X-ray photoelectron spectroscopy results. Multiple droplets were analyzed for each substrate.

A Topometrix (Explorer, TMX200) scanning probe microscope was used to examine the topography of dewet samples and to determine the "equilibrium contact" angles of dewet PS blend droplets on PMMA. Dewet droplets were analyzed after several hours of annealing when there were no further detectable changes in the drop shape. The contact angle was estimated by analysis of linear scans of probe height as a function of radial position across each droplet that were obtained using contact mode with a 100 μm SiN pyramidal tip. The effects of convolution of the tip geometry are expected to be small since the contact angles observed were small.

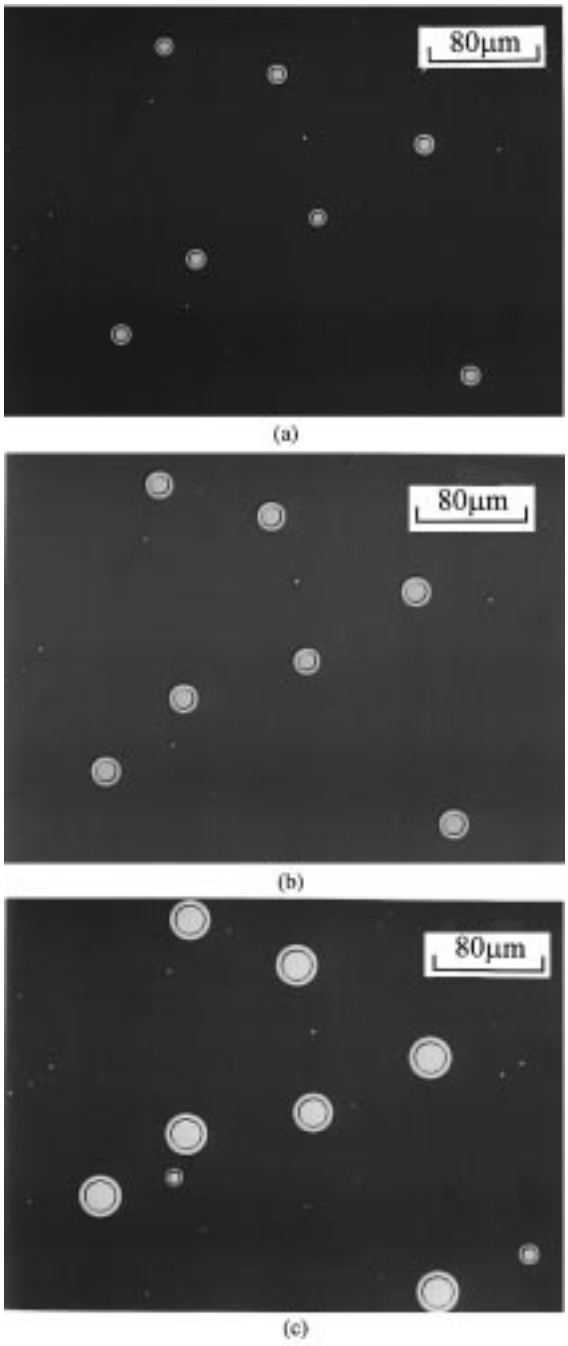

Figure 1. Optical micrographs showing the different stages of dewetting for a blend of PS−F17.3K 5% (w/w) with PS34.5K on PMMA100K after annealing at 165 °C for (a) 120, (b) 240, and (c) 420 min.

Results and Discussion

Typical optical photomicrographs of different stages of the dewetting process are shown in Figure 1 for a PS34.5K/PS−F17.3K (5% w/w) blend film on PMMA annealed at 165 °C for different times. The measured

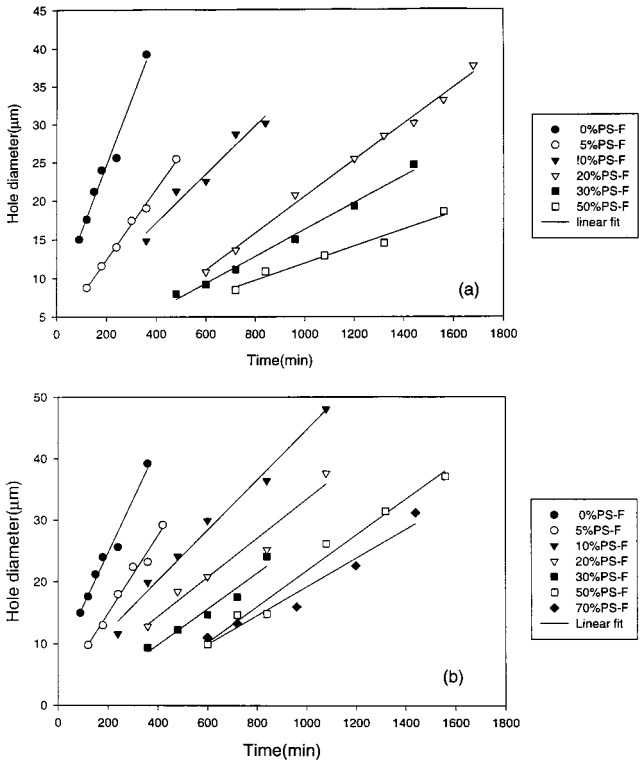

Figure 2. Hole diameter vs annealing time for blends (a) PS34.5K/ PS−F17.3K and (b) PS34.5K/PS−F35.5K as a function of the PS−F weight fraction.

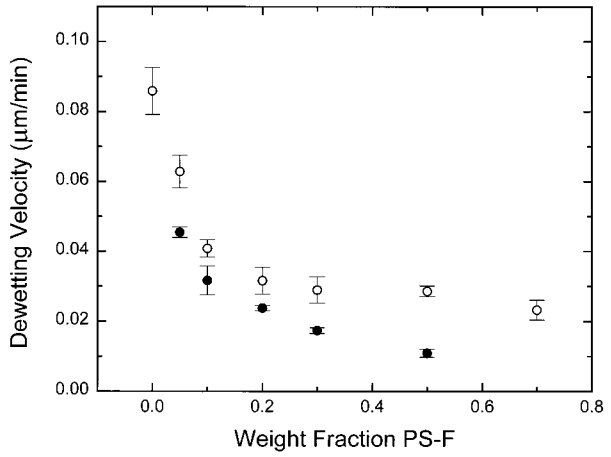

Figure 3. Dewetting velocity as a function of weight fraction of PS−F17.3K (filled circles) and PS−F35.5K (open circles) blended with PS34.5K. The error bars indicate a range of two standard deviations.

hole diameters are reported in Figure 2 as a function of the bulk concentration of PS−F and the annealing time at 165 °C. Reported hole diameters represent averages over many holes measured from optical micrographs. Systematic studies for two low surface energy end-functional polystyrenes are presented: PS−F17.3K (Figure 2a) and PS−F35.5K (Figure 2b). The solid lines in the figure are the results of linear regression to the data. The figures demonstrate that PS dewets PMMA with a constant velocity and that the addition of fluorocarbon end-functional PS to the system has a strong influence on the dewetting velocity.

The dependence of dewetting velocity on the PS−F concentration in the PS blend is shown in Figure 3. The dewetting velocity initially decreases rapidly upon PS−F addition and more slowly as more PS−F is present. This behavior is a direct reflection of the surface absorption isotherm for the surface-active PS−F additives. At equal weight fraction, the lower molecular weight PS−F17.3K is more effective than the PS−F35.5K in decreasing the dewetting velocity. The film of neat PS−F35.5K did not dewet even after annealing at 165 °C for 3 days. Lower molecular weight additives impart higher stability due to the greater fluorocarbon content. In the case of PS−F17.3K, a blend containing 70% PS−F was stable after annealing at 165 °C for 3 days. When an even lower molecular weight material (PS−F5.4K) of molecular weight 5400 was used (data not shown), a film containing only 50% of the additive was stable under these same conditions.

BMR[1] presented a theoretical treatment of dewetting for a liquid(A)/liquid(B) bilayer system. The lower layer behaves like a solid when $\eta_B > \eta_A/\theta_E$ where η_B and η_A are the viscosities of liquid A and B, respectively, and θ_E is the equilibrium contact angle of liquid A on liquid B. If θ_E is small, the dewetting velocity is predicted to be independent of time and can be described as

$$V = \frac{1}{12L\sqrt{2}}\frac{\gamma_A}{\eta_A}{\theta_E}^3 \qquad (2)$$

where γ_A is the surface tension of liquid A and L is a logarithmic factor of order 10 and is due to a divergence of the dissipation in a wedge. The condition $\eta_B > \eta_A/\theta_E$[15] is satisfied for the PS blends on PMMA, and the small-angle assumption is valid for our experiments (see data in Table 2), so that (2) can be compared directly to experimental dewetting velocities. The predicted time invariance of dewetting velocity is confirmed by the data in Figure 2 that show a linear dependence of hole diameter on time.

Application of the theory to model the dependence of dewetting velocity on the concentration and molecular weight of the PS−F additive (see Figure 3) requires knowledge of how the surface tension of the blend, γ_A, its equilibrium contact angle on PMMA, θ_E, and its melt viscosity, η_A, depend on blend composition and additive molecular weight. Figure 4 shows room-temperature contact angles for water droplets placed on blends of PS and PS−F that were previously annealed at 165 °C for 30 min. The water contact angle is an increasing function of PS−F weight fraction, ϕ_{PS-F}, indicating that the surface tension of the blends decreases with bulk weight fraction of PS−F. The contact angle is not linear in PS−F fraction due to preferential surface segregation of the lower surface energy PS−F. That is, PS−F acts as a surfactant. Within certain assumptions, the water contact angle data can be used to estimate the surface tensions of the polymer blends. These calculations and a detailed treatment of the adsorption isotherms of the blends are presented in a paper to follow.[29] While at a particular blend composition the contact angles for the two molecular weight additives are within experimental error, the overall molecular weight trend is evident; the average contact angles for the lower molecular weight PS−F17.3K blends are all higher, consistent with an expected higher fluorocarbon concentration at the surface.

For the purpose of the present paper, the blend surface tension is estimated from measurements of the equilibrium contact angle θ_E. AFM has been used to estimate the equilibrium contact angle of PS blend droplets on the PMMA surface that form after dewetting

Table 2. Dewetting Velocity (v), Surface Tension[a] (γ_{PS}), Contact Angle on PMMA (θ_E), Viscosity[32] (η_{PS}), and ($\gamma_{PS}\theta_E^3/\eta_{PS}$) for Blends of PS-F17.3K and PS-F35.5K with PS-34.5K as a Function of the Blend Composition; Cited Errors Indicate One Standard Deviation

wt % PS-F	v, μm/min	γ_{PS}, dyn/cm	θ_E, deg	η_{PS}, P	$\gamma_{PS}\theta_E^3/\eta_{PS}$, μm/min
			PS-F17.3K		
0	0.086 ± 0.007	29.22 ± 7.88	11.3 ± 1.4	1.15×10^4	11.7 ± 4.0
5	0.046 ± 0.0015	20.04 ± 3.56	9.5 ± 0.7	1.07×10^4	7.3 ± 1.3
10	0.032 ± 0.004	28.95 ± 3.92	8.3 ± 1.1	9.91×10^3	5.3 ± 1.3
20	0.024 ± 0.0007	28.85 ± 1.94	6.7 ± 0.6	8.47×10^3	3.4 ± 0.5
30	0.017 ± 0.0008	28.80 ± 1.38	5.9 ± 0.5	7.19×10^3	2.6 ± 0.4
50	0.011 ± 0.001	28.74 ± 2.87	4.5 ± 1.3	5.04×10^3	1.7 ± 0.8
			PS-F35.5K		
0	0.086 ± 0.007	29.22 ± 7.88	11.3 ± 1.4	1.15×10^4	11.7 ± 4.0
5	0.063 ± 0.005	29.13 ± 9.77	10.4 ± 1.8	1.16×10^4	9.2 ± 4.1
10	0.041 ± 0.002	29.02 ± 4.78	9.2 ± 1.0	1.16×10^4	6.2 ± 1.6
20	0.032 ± 0.004	28.94 ± 2.28	8.1 ± 0.6	1.16×10^4	4.3 ± 0.6
30	0.029 ± 0.004	28.83 ± 2.38	6.5 ± 0.7	1.18×10^4	2.1 ± 0.4
50	0.029 ± 0.0015	28.80	5.8	1.20×10^4	1.5
70	0.023 ± 0.003	28.79 ± 0.47	5.7 ± 0.2	1.21×10^4	1.4 ± 0.07

[a] Estimated from eq 4.

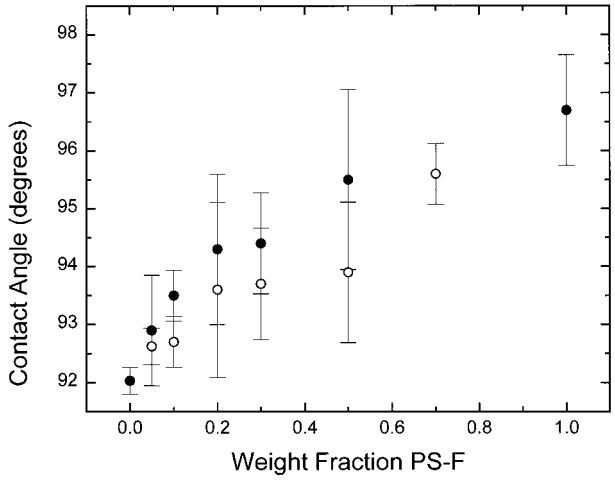

Figure 4. Contact angle of water on PS blend films as a function of the weight fraction of PS−F17.3K (filled circles) and PS−F35.5K (open circles) blended with PS34.5K (after annealing at 165 °C for 30 min). The error bars indicate a range of two standard deviations.

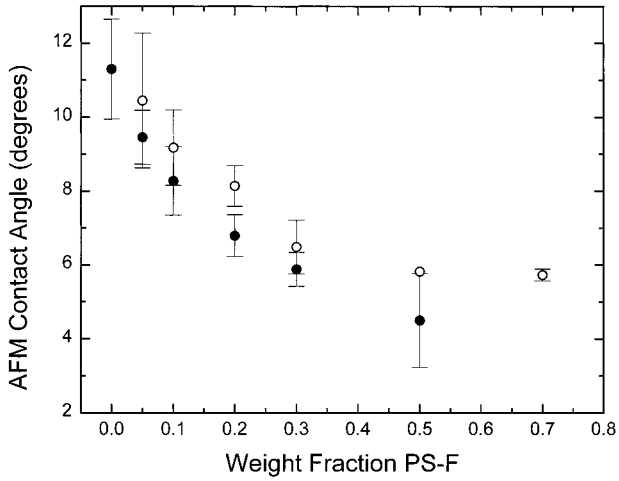

Figure 5. Contact angle of dewet PS blend droplets on PMMA substrates measured by AFM, as a function of the bulk weight fraction of PS−F17.3K (filled circles) and PS−F35.5K (open circles) blended with PS34.5K (after annealing at 165 °C for 3 days). The error bars indicate a range of two standard deviations.

at 165 °C for more than 3 days. The contact angle was obtained from AFM measurements of the drop height, H, and the drop radius, R, and calculated as follows:[30]

$$\tan(\theta_E/2) = H/R \tag{3}$$

In applying (3), the measured value of height, H, was multiplied by a factor 0.93 to account for contraction of polystyrene after being quenched from 165 °C to room temperature, and we assume that the volume contraction of PMMA is similar to that of PS, so that the value of R is unchanged. Figure 5 shows the equilibrium contact angle, θ_E, as a function of bulk weight fraction of PS−F in the blend. For addition of PS−F35.5K, which has a similar molecular weight as PS34.5K, the equilibrium contact angle decreases almost linearly with weight fraction of PS−F present in the system and reaches a plateau at about 20% weight fraction. The addition of PS−F17.3K to the PS34.5K matrix leads to a decrease in the equilibrium contact angle that is statistically larger than that for most of the PS−F35.5K blends, and the decrease persists to larger volume fraction of PS−F. The larger decrease in contact angle is consistent with water contact angle results and indicates stronger adsorption of lower molecular weight PS−F as a result of its higher relative fluorocarbon content.

The surface tension of the PS blends with PS−F can be estimated from a force balance of dewet PS droplets on the PMMA surface through Young's equation

$$\gamma_{PS} = \frac{\gamma_{PMMA} - \gamma_{PMMA/PS}}{\cos\theta_E} \tag{4}$$

where γ_{PMMA}, γ_{PS}, and $\gamma_{PMMA/PS}$ are the surface tension of PMMA, PS, and interfacial tension between PMMA and PS, respectively. We take values of $\gamma_{PMMA} = 30.1$ dyn/cm and $\gamma_{PMMA/PS} = 1.45$ dyn/cm at 165 °C from the literature[31] and assume that the fluorocarbon end groups do not significantly influence the interfacial tension. The resultant surface tensions for the blends at 165° C estimated in this fashion are reported in Table 2.

The final parameter required for application of (2) is the melt viscosity of the blends of PS and PS−F. To estimate the viscosity of the PS blends, we neglect the influence of end groups on the viscosity, as the bulk concentration of end group is very low (less than 1%), and use empirical expressions to account for the mo-

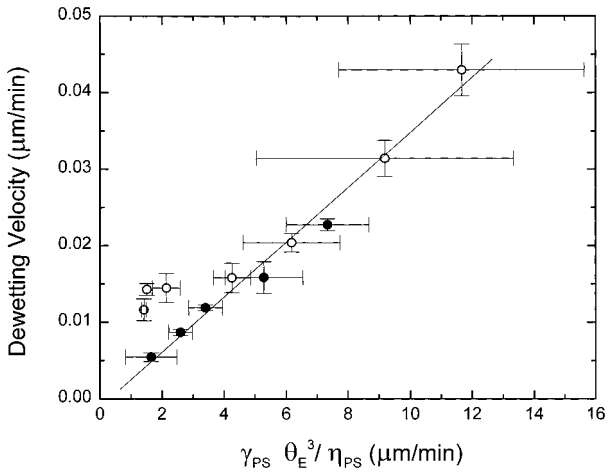

Figure 6. Dewetting velocity vs $\gamma_{PS}\theta_E^3/\eta_{PS}$ for blends of PS−F17.3K (filled circles) and PS−F35.5K in (open circles) with PS34.5K. The error bars indicate a range of two standard deviations.

lecular weight[32] and temperature dependence[33] of PS viscosity. The melt viscosities of the pure components estimated from these relations are 1.15×10^4, 0.17×10^4, and 1.25×10^4 P respectively for PS34.5K, PS−F17.3, and PS−F35.5K at the experimental temperature of 165 °C. The viscosity of each blend was estimated from an empirical mixing rule.[34]

The calculated values of γ_{PS}, η_{PS}, and $\gamma_{PS}\theta_E^3/\eta_{PS}$ for the PS−F17.3K and PS−F35.5K blends are listed in Table 2 along with relevant standard deviations. The equilibrium contact angles measured are sufficiently small to warrant applicability of the small-angle assumption intrinsic to (2). A plot of the dewetting velocity as a function of $\gamma_{PS}\theta_E^3/\eta_{PS}$ as suggested by (2) is shown in Figure 6. Both data sets follow a linear relationship that is well represented by a single solid line in the figure. The dewetting velocity is found to be directly proportional to $\gamma_{PS}\theta_E^3/\eta_{PS}$, in accordance with the prediction of the BMR theory. Three data points at the highest weight percent of PS−F35.5K deviate slightly from this behavior and were not considered in the regression of the line. The deviation of these data may be associated with the saturation effect seen in Figure 5, since the equilibrium contact angle has the greatest influence on the dewetting velocity. Analysis of the slope of the solid line yields a value of $L = 16.4 \pm 0.1$. This compares well to previously reported values for poly(dimethylsiloxane)[35] that fell within the range 9.0−19.7.

Summary

We demonstrate that poly(styrene) with a low-energy fluorocarbon end group (PS−F) is a useful and effective additive for the control and in certain cases the elimination of dewetting for thin films of nonfunctional poly(styrene) on poly(methyl methacrylate) substrates. The dewetting velocity, determined by microscopic measurement of hole growth, is found to be time invariant and decreases upon addition of PS−F. In the case of neat PS−F, the films are stable indefinitely. Increased film stability is the result of the decrease in surface tension (characterized by contact angle analysis) brought about by the addition of PS−F. Lower molecular weight PS−F is more effective in suppressing dewetting owing to its higher fluorocarbon content and a subsequently lower surface tension. The dependence of dewetting velocity on melt viscosity, surface tension, and contact angle is in excellent agreement with the theoretical predictions by Brochard-Wyatt, Martin, and Redon.

Acknowledgment. This material is based upon work supported by, or in part by, the U.S. Army Research Office and Grant DAAH04-95-1-0592 and the National Science Foundation (DMR-9502977 and DMR-9810069).

References and Notes

(1) Brochard-Wyart, F.; Martin, P.; Roden, C. *Langmuir* **1993**, *9*, 3682.
(2) Dan, N. *Langmuir* **1996**, *12*, 1101.
(3) Brochard-Wyart, F.; Debregeas, G.; Martin, P. *Macromolecules* **1997**, *30*, 1211.
(4) Martin, J. I.; Wang, Z. G. *Langmuir* **1996**, *12*, 4950.
(5) Shull, K. R. *Macromolecules* **1996**, *29*, 8487.
(6) Gay, C. *Macromolecules* **1997**, *30*, 5939.
(7) Reiter, G. *Phys. Rev. Lett.* **1992**, *68*, 75.
(8) Zhao, W.; Rafailovich, M. H.; Sokolov, J. *Phys. Rev. Lett.* **1993**, *70*, 1453.
(9) Redon, C.; Brzoska, J. B.; Brochard-Wyart, F. *Macromolecules* **1994**, *27*, 468.
(10) Genzer, J.; Kramer, E. J. *Phys. Rev. Lett.* **1997**, *78*, 4946.
(11) Kerle, T.; Yerushalmi-Rozen, R.; Klein, J. *Europhys. Lett.* **1997**, *38*, 207.
(12) Reiter, G.; Avroy, P.; Auray, L. *Macromolecules* **1996**, *29*, 2150.
(13) Silberzan, P.; Leger, L. *Macromolecules* **1992**, *25*, 1267.
(14) Faldi, A.; Composto, R. J.; Winey, K. I. *Langmuir* **1995**, *11*, 4855; **1997**, *13*, 1758.
(15) Qu, S.; Darke, C. J.; Liu, Y.; Rafailovich, M. H.; Sokolov, J.; Phelan, K. C.; Krausch, G. *Macromolecules* **1997**, *30*, 3640.
(16) Henn, G.; Bucknall, D. G.; Stamm, M.; Vanhoorne, P.; Jerome, R. *Macromolecules* **1996**, *29*, 4305.
(17) Yerushalmi-Rozen, R.; Klein, J. *Langmuir* **1995**, *11*, 2806.
(18) Schaulb, T. F.; Kellogy, G. J.; Mayes, A. M. *Macromolecules* **1996**, *29*, 3982.
(19) Iyengar, D. R.; Perutz, S. M.; Dai, Chi-An; Ober, C. K.; Kramer, E. J. *Macromolecules* **1996**, *29*, 1229.
(20) Lenk, T. J.; Lee, D. H. T.; Koberstein, J. T. *Langmuir* **1994**, *10*, 1857.
(21) Jalbert, C.; Koberstein, J. T.; Hariharan, A.; Kumar, K. *Macromolecules* **1997**, *30*, 4481.
(22) Jalbert, C.; Koberstein, J. T.; Yilgor, I.; Gallagher, P.; Krukonis, V. *Macromolecules* **1993**, *26*, 3069.
(23) Elman, J.; Johs, B.; Long, T.; Koberstein, J. T. *Macromolecules* **1994**, *27*, 5341.
(24) Affrossman, S.; Hartshorne, M.; Kiff, T.; Pethrick, R. A.; Richards, R. W. *Macromolecules* **1994**, *27*, 1588.
(25) Hunt, M. O. J.; Belu, A. M.; Linton, R. W.; Desimone, J. M. *Macromolecules* **1993**, *26*, 4854.
(26) Schaulb, T. F.; Kellogy, G. J.; Mayes, A. M.; Kulasekere, R.; Anker, J. F.; Kaiser, H. *Macromolecules* **1996**, *29*, 3982.
(27) Chen, J.-K.; Koberstein, J. T.; Siegel, A. F.; Sohn, J. E.; Emerson, J. A. *J. Colloid Interface Sci.* **1987**, *l19*, 55.
(28) Jalbert, C. J. Ph.D. Dissertation, University of Connecticut, 1993.
(29) Yuan, C.; O'Rourke, P.; Baetzold, J. P.; Koberstein, J. T., manuscript in preparation.
(30) Vitt, E.; Shull, K. R. *Macromolecules* **1995**, *28*, 6349.
(31) Wu, S. *Polymer Interface and Adhesion*; Marcel Dekker: New York, 1982.
(32) See eq 5 in: Fox, T. G.; Flory, P. J. *J. Phys. Chem.* **1951**, *55*, 221.
(33) Fox, T. G.; Flory, P. J. *J. Appl. Phys.* **1950**, *21*, 581.
(34) The viscosity of each two-component blend was estimated from the relation $\eta^{1/\alpha} = w_1\eta_1^{1/\alpha} + w_2\eta_2^{1/\alpha}$ where w_i is the weight fraction of each component and $\alpha = 2.0$ as proposed by Menefee (Menefee, E. J. *Appl. Polym. Sci.* **1972**, *16*, 2215) and discussed by Liu et al. (Liu, Y.; Shaw, M. T. *J. Rheol.* **1998**, *42* (2), 267).
(35) Redon, C.; Brochard-Wyatt, F.; Rondelez, F. *Phys. Rev. Lett.* **1991**, *66*, 715.

MA980774O